MATERIALS CHEMISTRY FRONTIERS

RESEARCH ARTICLE

View Article Online
View Journal | View Issue

Cite this: *Mater. Chem. Front.*, 2021, **5**, 7032

Highly sensitive detection of paraquat with pillar[5]arenes as an aptamer in an α-hemolysin nanopore†

Xiaojia Jiang,[a] Mingsong Zang,[a] Fei Li,[a] Chunxi Hou,[a] Quan Luo,[a] Jiayun Xu[b] and Junqiu Liu *[ab]

Received 16th June 2021,
Accepted 5th August 2021

DOI: 10.1039/d1qm00875g

rsc.li/frontiers-materials

Recently, biological nanopore-based techniques have attracted more and more attention in the field of single-molecule detection because they allow real-time, sensitive, high-throughput analysis. Herein, we report an engineered biological nanopore sensor by introducing a macrocyclic host molecule carboxylatopillar[5]arene (CP[5]A) that acts as an aptamer into the lumen of a mutant $(E111R/K147R)_7$ αHL nanopore for detecting highly toxic paraquat (PQ) *via* host–guest interactions at the single-molecule level. By taking advantage of introducing positively charged arginine (Arg) into the lumen of the αHL nanopore, our engineered nanopore sensor exhibits higher stability. More importantly, this nanopore sensor shows high sensitivity, and the limit of detection (LOD) for PQ can reach a nanomolar level of 0.37 ppb. The CP[5]A-based nanopore sensing strategy developed in this work may bring inspiration for single-molecule detection and hold great potential in public health applications.

Introduction

In the past few decades, the invention and use of pesticides have greatly increased the yield of crops, but the environmental pollution caused by the excessive use of pesticides and the problem of pesticide residues in agricultural products have attracted more and more attention.[1] Among various pesticides, paraquat (PQ) is used widely; however, it is highly toxic to humans and animals. It is also highly water-soluble and easily absorbed by the skin and respiratory tract.[2,3] In particular, the mortality of PQ poisoning is high, and there are no obviously effective antidotes to it to date. However, we can alleviate the harm from paraquat by simply reducing its use and reinforcing its detection. The conventional analytical methods for pesticide detection include gas chromatography,[4] high-performance liquid chromatography,[5] fluorescent probes[6] and so on. These methods are highly selective and sensitive, but still suffer from disadvantages including expensive equipment, sophisticated requirements and time consumption. Therefore, it is of great importance and urgency to develop new efficient and sensitive techniques to detect PQ.

A stochastic sensor based on biological nanopores at the single-molecule level has developed rapidly in a myriad of fields[7–11] because they allow real-time, sensitive, high-throughput analysis. In principle, a nanopore sensor is a device that relies on the observation of individual binding events caused by the interaction between analytic molecules and the sensor elements in nanopores. By calculating the data originated from the binding events, we can obtain the changes of ionic current (ΔI), the mean inter-event interval (τ_{on}) and the mean duration time (τ_{off}) of analytes at a certain voltage. In addition, it is known that the frequency of the binding events ($1/\tau_{on}$) depends on the concentration of the analyte, while the identity of the analyte is determined by ΔI and τ_{off}. Based on these parameters, we can interpret the characteristics of analytes and then determine them. For instance, by genetic engineering and biochemical reactions, various engineered α-hemolysin (αHL) nanopores have been widely applied to detect a variety of matters ranging from ions,[12,13] molecules,[14,15] and nucleic acids,[16,17] to even chemical reactions[18,19] and so on at the single-molecule level. Meanwhile, supramolecular chemistry such as host–guest recognition also plays a vital role in the development of this field. For example, many research groups have combined the macrocyclic host molecule β-cyclodextrin (β-CD) and its derivatives that act as the aptamers with the αHL nanopore to detect some substances, such as copper ions,[13] nitrogen mustards[7] and enantiomers.[14] Besides β-CD, pillar[5]arene (P[5]A) has also attracted the attention of scientists recently, and is a relatively new supramolecular macromolecular

[a] *State Key Laboratory of Supramolecular Structure and Materials, College of Chemistry, Jilin University, Changchun 130012, China. E-mail: junqiuliu@jlu.edu.cn*
[b] *College of Material Chemistry and Chemical Engineering, Hangzhou Normal University, Hangzhou 311121, China*

† Electronic supplementary information (ESI) available. See DOI: 10.1039/d1qm00875g

host molecule first synthesized by Ogoshi.[20] Subsequently, it and its derivatives received considerable attention and were then applied in many fields,[21] such as nanomaterials,[22–24] molecular recognition,[25–27] ion transporting[28–30] and so on, because of their columnar structures,[31] easily modified rims and host–guest properties. Based on these unique properties, we anticipated that P[5]A could be used as an aptamer lodged in the lumen of the αHL nanopore for constructing a nanopore sensor to detect its guest molecules, such as PQ. Therefore, in this work, our group constructed an engineered nanopore by introducing water-soluble CP[5]A into the lumen of the mutant $(E111R/K147R)_7$ nanopore *via* non-covalent interaction. It is expected that this engineered nanopore, in which the CP[5]A acts as the aptamer, could detect PQ through host–guest interaction (Schemes 1 and 2). This work not only provides an approach for the detection of PQ at the single-molecule level, but also provides inspiration for the detection of other types of molecules based on our new nanopore sensor.

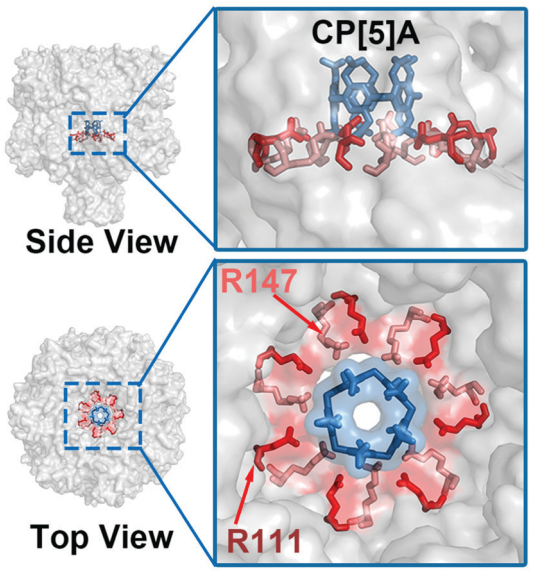

Scheme 2 Computer stimulation of the structures of the $(E111R/K147R)_7$ αHL nanopore and CP[5]A. The structure of the $(E111R/K147R)_7$ αHL nanopore was built by Pymol and the structure of CP[5]A was built by Gauss View and optimized by Gaussian 09.

Results and discussion

CP[5]A lodged in the mutant $(E111R/K147R)_7$ αHL nanopore

In order to lodge the P[5]A into the lumen of the αHL nanopore, we synthesized the water-soluble CP[5]A with five carboxyl groups on the upper and lower rims, according to the previous literature studies.[32] The synthetic route is shown in Scheme S1 (ESI†) and the characterization of CP[5]A sodium salts was performed by ^{1}H NMR (Fig. S1, ESI†). In addition, in this work, in order to strengthen the interaction between CP[5]A and the αHL nanopore, arginine (Arg) that contains positively charged side chains was introduced at the residues 111 and 147 of the αHL nanopore, respectively, by site-directed mutagenesis. In theory, the two mutated residues reside at the narrowest region of the αHL nanopore, which at 1.4 nm in diameter is the narrowest spot of αHL,[33] and thus interacts with CP[5]A more strongly. The mutant monomers self-assemble into a heptameric, mushroom-shaped nanopore on the bilayer membrane, bearing fourteen positive side chains stretching into the channel at the top of the transmembrane β-barrel. The purity and the molecular weight of the $(E111R/K147R)_7$ αHL nanopore were characterized by sodium dodecyl sulfate–poly acrylamide gel electrophoresis (SDS-PAGE) and MALDI-TOF mass spectrometry (Fig. S2 and S3, ESI†), respectively.

Experimentally, CP[5]A and the mutant $(E111R/K147R)_7$ αHL protein were added to the *cis* side of the chamber (the electrical ground side), respectively. The reason why we add the CP[5]A to the *cis* side of the chamber is that the CP[5]A is negatively charged and when driven by a positively successive applied voltage, the CP[5]A migrates through the nanopore. In theory, during the single-channel recording, when a proper interaction between the pore restriction and CP[5]A is established, single-molecule binding events can be observed. As expected, first, in

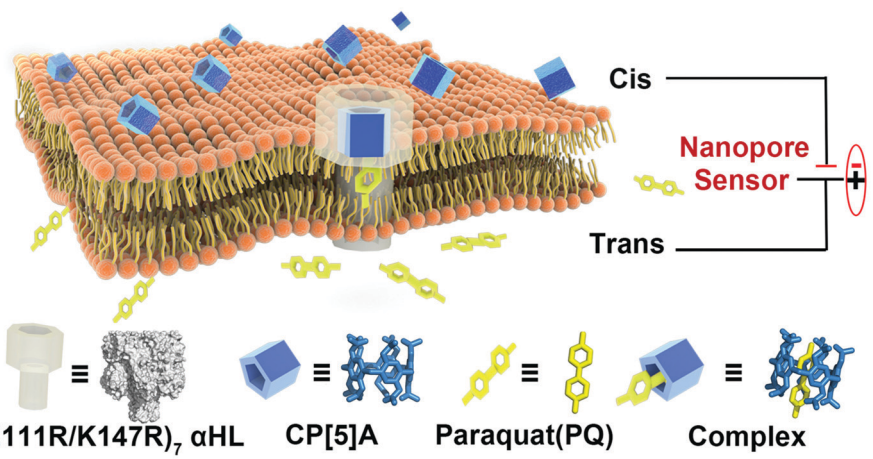

Scheme 1 A schematic of the new nanopore sensor for detecting paraquat (PQ) in which the CP[5]A acts as the recognition element introduced into the lumen of the $(E111R/K147R)_7$ αHL nanopore.

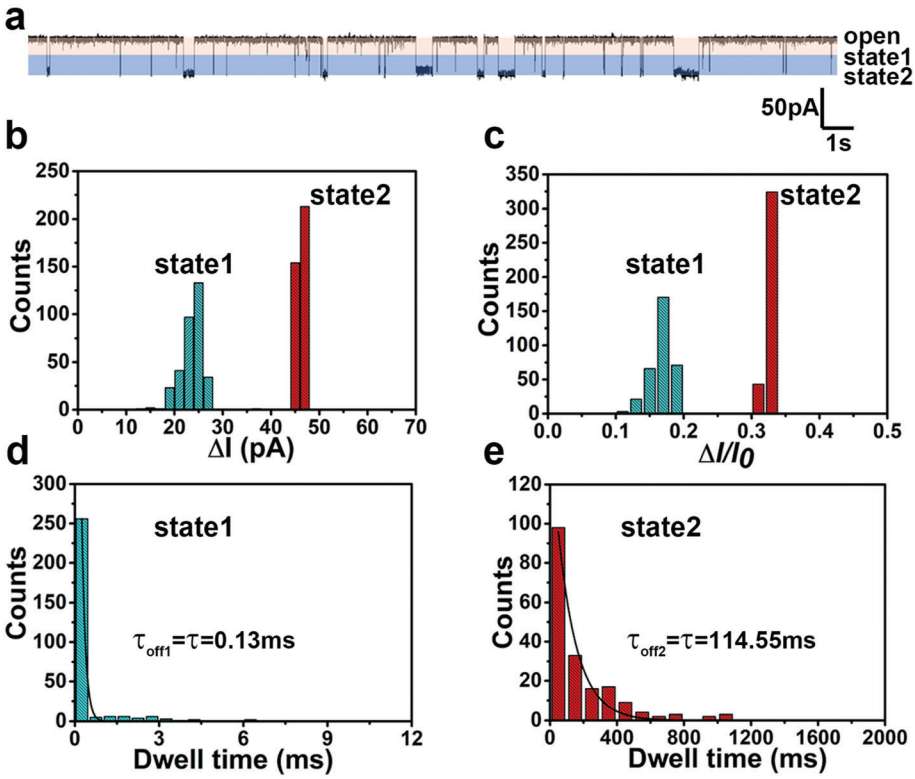

Fig. 1 Binding of CP[5]A within the $(E111R/K147R)_7$ αHL nanopore. (a) The current reduction amplitudes in the single $(E111R/K147R)_7$ αHL nanopore when 1 μM CP[5]A was added to the *cis* side at +100 mV. (b) An event histogram of ΔI for CP[5]A binding with the $(E111R/K147R)_7$ αHL nanopore. ΔI_{0-1} stands for the current difference between open and state1 and ΔI_{0-2} stands for the current difference between open and state2. (c) An event histogram of $\Delta I/I_0$ for CP[5]A binding with the $(E111R/K147R)_7$ αHL nanopore. $\Delta I_{0-1}/\Delta I_0$ and $\Delta I_{0-2}/\Delta I_0$ stand for the ratio of the current reduction between state1, state2 and open current. The histogram of the τ_{off} of CP[5]A from a series binding events. (d) The τ_{off1} of state1. (e) The τ_{off2} of state2.

the absence of CP[5]A, at the *cis* side, an open current of 140 ± 8 pA stayed a long time and no current reduction was observed at a +100 mV potential continuously applied. However, when the final concentration of 1 μM CP[5]A was added to the *cis* side of the chamber, after 10–20 minutes, successive binding events were clearly observed, in the form of two different reversible pore blockages (state1 and state2) (Fig. 1a), which exhibited shallow and deep current blockage values (ΔI), measuring 24 ± 3 pA (ΔI_{0-1} and $\Delta I_{0-1}/I_0$ = 0.17 ± 0.05) and 44 ± 2 pA (ΔI_{0-2} and $\Delta I_{0-2}/I_0$ = 0.33 ± 0.04) (Fig. 1b and c), respectively. Besides the current blockage values, there were also two distinct event dwell time (τ_{off}) values, including the shorter τ_{off} (τ_{off1} = 0.13 ± 0.04 ms) and the longer τ_{off} (τ_{off2} = 116.25 ± 0.05 ms) values, which were correlated to the current blockage values of 24 ± 3 pA (state1) and 44 ± 2 pA (state2), respectively (Fig. 1d and e). It should be noted that the current blockage ΔI_{0-1} and the dwell time τ_{off1} of state1 were relatively small, indicating that state1 was very unstable. One likely interpretation is that state1 was generated by partially binding or the collision between CP[5]A and the lumen of the αHL nanopore.

To further examine whether the binding events of state2 were contributed by the binding between CP[5]A and the restriction of the $(E111R/K147R)_7$ αHL nanopore *via* the non-covalent interaction, a series of single-channel bilayer experiments were carried out with the different concentrations of CP[5]A. Experimentally, after the successful insertion of a single nanopore, the CP[5]A solution was added to the *cis* compartment. The accumulated final concentrations were 2.5 μM, 5 μM and 10 μM, respectively, and we found that the current blockages stayed at the same level in spite of the fact that the concentration of CP[5]A was accumulated (Fig. 2 and Fig. S4, ESI†). Quantitatively, the mean inter-event interval (τ_{on}) and the dwell time (τ_{off}) in different concentrations of CP[5]A (2.5 μM, 5 μM and 10 μM) were derived from the single exponential fitting result (Fig. 3a and b). Then, it should be noted that the reciprocal of the τ_{on} is proportional to the CP[5]A

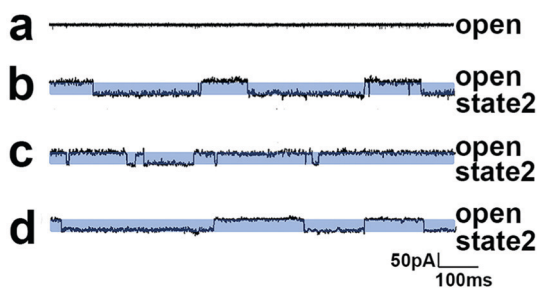

Fig. 2 Representation of the characteristic current blockages of different concentrations of CP[5]A. (a) The open current of the $(E111R/K147R)_7$ αHL nanopore; (b–d) the current blockages of 2.5 μM, 5 μM and 10 μM CP[5]A added to the *cis* side, respectively, at +100 mV.

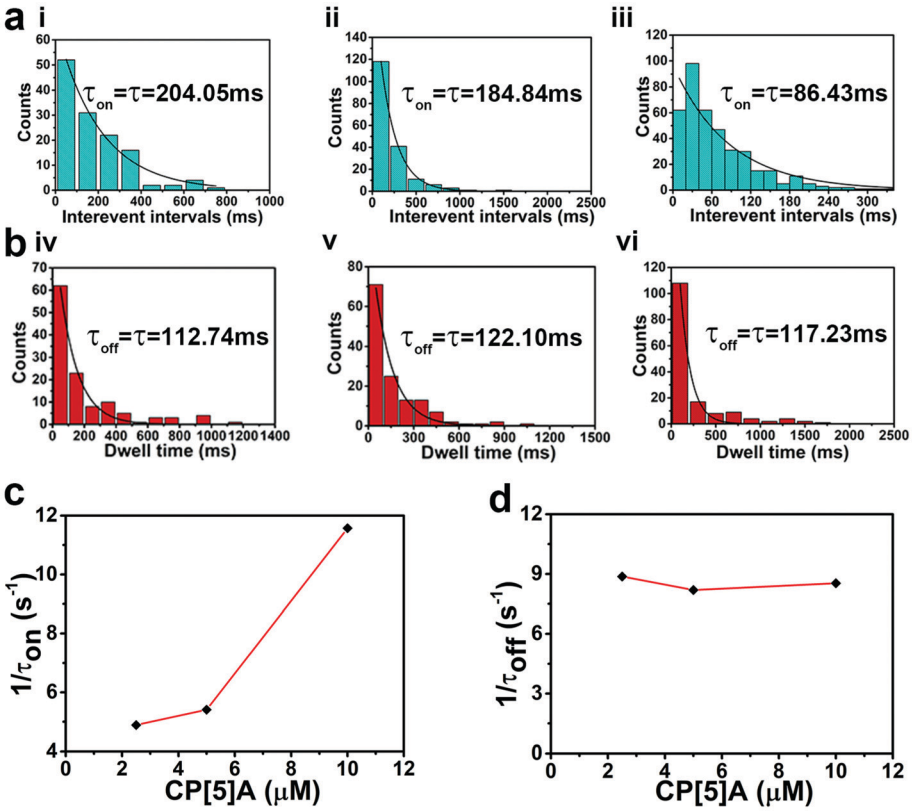

Fig. 3 (a and b) The τ_{on} and τ_{off} for CP[5]A-binding events with different concentrations of CP[5]A. (i and iv) represent the τ_{on} and τ_{off} value of 2.5 μM CP[5]A; (ii and v) represent the τ_{on} and τ_{off} value of 5 μM CP[5]A; and (iii and vi) represent the τ_{on} and τ_{off} value of 10 μM CP[5]A, respectively. The statistical data were obtained from a continuous 60 min recording. (c and d) The plot of the reciprocal of τ_{on} and the plot of the reciprocal of τ_{off} for CP[5]A-binding events *versus* the CP[5]A concentration.

concentration (Fig. 3c), which means that the frequency of the binding events clearly increased with the accumulating concentration of CP[5]A. Meanwhile, the relationship between $1/\tau_{on}$ and concentration is consistent with a bimolecular model, in which $1/\tau_{on} = k_{on}$[CP[5]A] and k_{on} is the association constant. In contrast, the relationship between the τ_{off} and the CP[5]A concentration has a near zero slope (Fig. 3d), which is consistent with a unimolecular dissociation mechanism ($1/\tau_{off} = k_{off}$ and k_{off} is the dissociation constant). Therefore, the forward and reverse rate constants derived from the τ values ($k_{on} = (1.49 \pm 0.47) \times 10^6$ M^{-1} s^{-1} and $k_{off} = (8.5 \pm 0.2)$ s^{-1}) yield a formation constant of $K_d = (6.70 \pm 2.26) \times 10^{-5}$ M ($K_d = k_{on}/k_{off}$) at 25 °C (Table S1, ESI†), indicating that the CP[5]A can be stably bound within the restriction of the $(E111R/K147R)_7$ αHL nanopore *via* non-covalent interaction.

The control experiment of CP[5]A lodged into the wild-type αHL nanopore

In order to confirm that introducing positively charged chains into the lumen of the nanopore can tighten the binding between CP[5]A and the nanopore, we also tested the binding between CP[5]A and the wild-type αHL nanopore (Fig. S5, ESI†). As we expected, there were still two distinct states, which included state1 and state2, when 1 μM CP[5]A was added to the *cis* side and the corresponding current blockage values of state1 ($\Delta I_{0-1}/I_0 = 0.16 \pm 0.08$) (Fig. 4a) and state2 ($\Delta I_{0-2}/I_0 = 0.34 \pm 0.03$) (Fig. 4c) were similar to those of the mutant $(E111R/K147R)_7$ αHL nanopore lodged with CP[5]A. In addition, it should be noted that the τ_{off2} value of the wild-type αHL nanopore lodged with CP[5]A was 72.25 ± 0.05 ms (Fig. 4d and Fig. S6b, ESI†), which is shorter than the τ_{off2} value (τ_{off2} = 116.25 ± 0.05 ms) of the $(E111R/K147R)_7$ αHL nanopore, proving that the positively charged chains introduced into the lumen of the αHL nanopore definitely improved the binding between CP[5]A and the restriction of the nanopore. On the other hand, the τ_{off1} value of the wild-type αHL nanopore (0.25 ± 0.05 ms) (Fig. 4b and Fig. S6c, ESI†) was similar to that (τ_{off1} = 0.13 ± 0.04 ms) of the mutant $(E111R/K147R)_7$ αHL nanopore, indicating that state1 was contributed by the unstable and random collision between CP[5]A and the nanopore. In particular, considering that state1 was generated by the unstable and random collision between CP[5]A and the αHL nanopore, it is necessary to ignore state1 to simplify the process of analysing the data. Hence, the characteristic binding state of CP[5]A lodged into the nanopore is referred to as state2 in the following analysis.

Direct detection of PQ based on the CP[5]A binding within the $(E111R/K147R)_7$ αHL nanopore

Since we have constructed a new nanopore by attaching CP[5]A into the restriction of the αHL nanopore, we anticipate that this

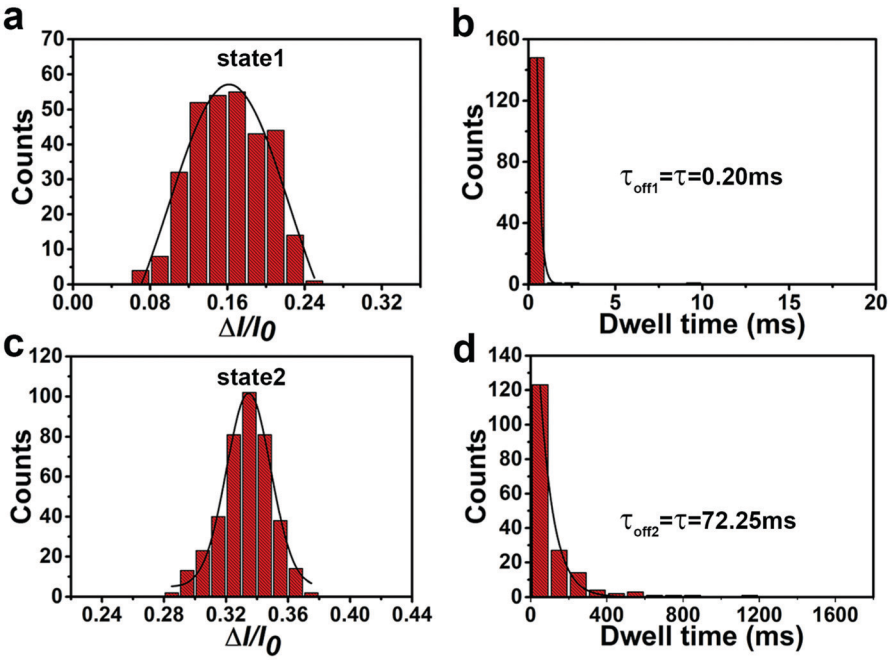

Fig. 4 (a) Event histogram of state1 for 1 μM CP[5]A binding with the wild-type αHL nanopore, $\Delta I_{0-1}/\Delta I_0 = 0.16 \pm 0.08$; (b) the τ_{off1} of state1; (c) the event histogram of state2 for CP[5]A binding with the wild-type αHL nanopore, $\Delta I_{0-2}/I_0 = 0.34 \pm 0.03$; and (d) the τ_{off2} of state2. The mean dwell times of state1 and state2 were obtained from the single exponential fitting result, and $\Delta I_{0-1}/\Delta I_0$ and $\Delta I_{0-2}/\Delta I_0$ stand for the ratio of the current reduction between state1, state2 and open current, respectively. The statistical data were obtained from a continuous 30 min recording.

engineered nanopore could be applied in the field of stochastic detection. It is well known that the host molecule-P[5]A could recognize the guest molecule, such as PQ. Hence, we examined the interaction between CP[5]A and PQ, that is, positively charged PQ can form a complexation with negatively charged CP[5]A *via* host–guest interaction as well as their thermodynamic parameters by ITC (Fig. S7, ESI†). The association constant (K_a) between CP[5]A and PQ was determined to be 1.01×10^7 M^{-1} in 1 : 1 complexation, indicating that the cavity of CP[5]A can accommodate one PQ moiety and the K_a value is relatively high, which laid the foundation for utilizing the host molecule CP[5]A that can act as the aptamer introduced into the lumen of the nanopore to recognize its guest molecule PQ.

Then, to test the feasibility of utilizing the CP[5]A-based nanopore to detect the guest molecule PQ, a series of single-channel recordings were carried out. Experimentally, CP[5]A was added to the *cis* side and PQ was added to the *trans* side with 5 μM and 1 μM in concentration. The reason for adding PQ and the CP[5]A to the opposite sides of the pore is that they are oppositely charged. Therefore, at a positive potential, CP[5]A can be bound to the nanopore under the action of the electrophoretic force, and the positively charged PQ was driven from the *trans* side to the *cis* side. Fortunately, from the electrophysiological recording, a new state (state3) was observed when the PQ was added to the *trans* side, which could be clearly distinguished from state2 when CP[5]A was the sole molecule added (Fig. 5a and b). Then, by calculating the current blockage values and the τ_{off} value of state3, we concluded that the histogram of $\Delta I_{2-3}/I_0$ (0.48 ± 0.03) was totally different from that of $\Delta I_{0-2}/I_0$ (0.34 ± 0.03), indicating that state3 was contributed to the recognition between CP[5]A and PQ (Fig. 5d). In addition, the τ_{off} value of state3 was derived as 9.91 ± 0.16 ms (Fig. 5e). Based on the properties of host–guest chemistry, the recognition between CP[5]A and PQ could be regarded as a reversible interaction. Accordingly, we observed that state2 turned into state3 when CP[5]A captured PQ, and then state3 turned into state2 or state1 when PQ dissociated from CP[5]A (Fig. 5c), which should be attributed to the host–guest recognition between CP[5]A and PQ. As discussed above, our engineered nanopore sensor in which CP[5]A acted as the aptamer could be used to detect PQ at the single-molecule level.

Detection limit for PQ

Next, in order to investigate the sensitivity of our engineered αHL nanopore sensor in which CP[5]A acted as the aptamer for detecting PQ, a series of PQ solutions were prepared with different concentrations and then detected by our nanopore sensor. By analysing the characteristic binding events of state3 with different concentrations (2 nM, 4 nM, 1 μM, 20 μM and 50 μM), we calculated the τ_{off3} values under these concentrations (Fig. 6a–e). It should also be noted that the $1/\tau_{off}$ values of state3 hardly changed with the accumulation of the PQ concentration (Fig. 6f), indicating that the same type of binding event was observed in different PQ concentrations. Importantly, the characteristic current blockage of state3 could only be detected over the concentration of 2 nM PQ (Fig. S8, ESI†), showing that our nanopore sensor can detect PQ at concentrations as low as 2 nM. In addition, the LOD value for detecting PQ based on our

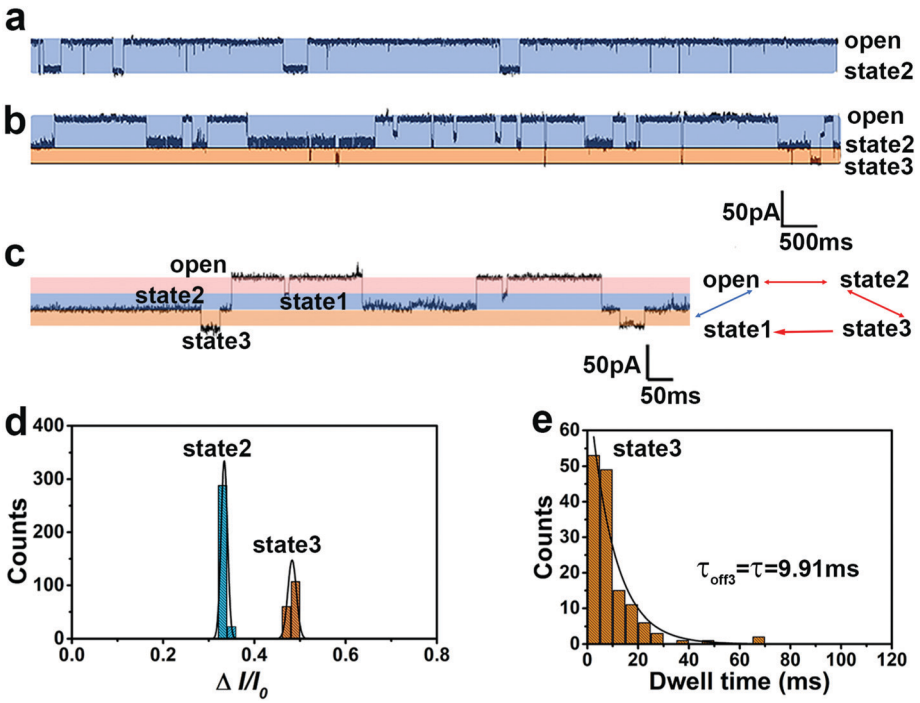

Fig. 5 The characteristic current reduction amplitudes when CP[5]A was added to the *cis* side and PQ was added to the *trans* side. (a) The current reduction when CP[5]A was the sole molecule; (b) the current reduction when CP[5]A was added to the *cis* side and PQ was added to the *trans* side. (c) The enlarged view of the part of the current in Fig. b. (d) The stochastic sensing of PQ: the event histogram of CP[5]A and PQ, $\Delta I_{0-2}/\Delta I_0 = 0.34 \pm 0.03$; $\Delta I_{0-3}/\Delta I_0 = 0.48 \pm 0.03$; and $\Delta I_{0-2}/\Delta I_0$ and $\Delta I_{0-3}/\Delta I_0$ stand for the ratio of the current reduction between state2, state3 and open current. (e) The histogram of the τ_{off} of PQ added to the *trans* side and 5 μM CP[5]A added to the *cis* side. The statistical data in (d and e) were obtained from a continuous 30 min recording.

nanopore sensor was estimated to be 0.37 ppb, which was below the maximum residue limits (MRL) for PQ in food (PQ: 62.5 ppb) according to the National Food Safety Standard of China (GB 2763.1-2018). Compared to the reported detection methods, such as fluorescence sensing, high-performance liquid chromatography and capillary electrophoresis, our αHL nanopore sensor in which P[5]A acted as the aptamer to detect PQ shows higher sensitivity and holds great potential in public health applications.

Experimental

Materials

All solvents used in the experiments were obtained from Beijing Chemical Plant. 1,2-Diphytanoyl-*sn*-glycero- 3-phosphocholine (DPhPC) was from Avanti Polar Lipids. 4-(2-Hydroxyethyl)-1-piperazineethanesulfonic acid (HEPES), decane and Triton X-100 were from Sangon Biotech. *E. coli* strain BL21 (DE3) was from Tiangen Biotech. PQ was purchased from Aladdin Co. Isopropyl β-D-1-thiogalactopyranoside (IPTG) was purchased from Solarbio.

The preparation of CP[5]A

CP[5]A was synthesized according to a modified procedure. To a solution of 1,4-dimethoxybenzene (2.79 g, 20 mmol) and paraformaldehyde (1.96 g, 60 mmol) in dry 1,2-dichloroethane (180 mL), boron trifluoride etherate (2.4 mL, 20 mmol) was added under a nitrogen atmosphere. The mixture was stirred at room temperature. Subsequently, methanol (350 mL) was poured into the solution and the filter cake was collected by filtration. The product a (2 g, 2.7 mmol) obtained in the previous step was dissolved in dry chloroform (150 mL) solution and then boron tribromide (5 mL, 53 mmol) was added. The mixture was stirred at room temperature. After the reaction was complete, deionized water (300 mL) was added to obtain a precipitate (white); the reactants were stirred for another 2 hours and then filtered to collect the precipitate, which was washed with dilute hydrochloric acid solution (50 mL, 1 M) and chloroform (20 mL) to obtain product b. Subsequently, under the protection of nitrogen, product b (2.50 g, 4.1 mmol) was dissolved in acetonitrile (150 mL) containing potassium carbonate (7.00 g, 50 mmol) and potassium iodide (30 mg, 0.2 mmol), and stirred for 20 minutes. Then, an excess amount of ethyl bromoacetate ester (11.00 mL, 99 mmol) was added and the mixture was heated to reflux at 86 °C for 24 hours to obtain product c. Finally, product c was hydrolysed in a mixed medium that contained methanol/tetrahydrofuran (1 : 3) and sodium hydroxide to obtain the desired product d (white powder).

Construction, expression and purification of the (E111R/K147R)$_7$ αHL protein

Based on the computational stimulation, we mutated the residues 111 and 147 of the αHL to arginine (Arg) sequentially through

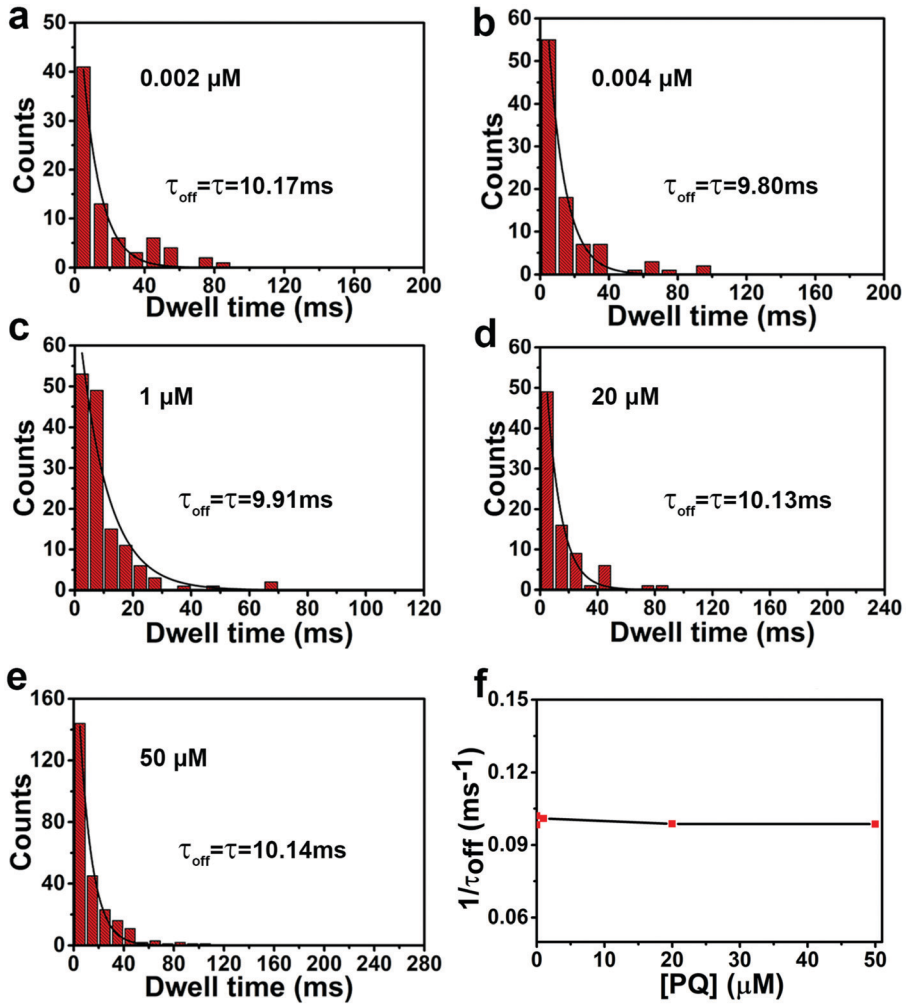

Fig. 6 Investigation of the detection limit for PQ detection. (a–e) The histogram of the dwell time of state3 (τ_{off3}, PQ) from a series of PQ-binding events with different concentrations. The τ_{off} was derived from the single exponential fitting result. The statistical data in (a–e) were obtained from a continuous 10 min recording. (f) The plot of the reciprocal of τ_{off} for PQ-binding events *versus* PQ concentration.

site-directed mutagenesis. The primers used in PCR were synthesized by Sangon Biotech. The mutated plasmids were testified by DNA sequencing and then transformed into *Escherichia coli* BL21 (DE3) for protein expression. The *E. coli* BL21 (DE3) strain containing a $(E111R/K147R)_7$ αHL gene was cultured in 1L LB (Luria broth) medium containing 100 μg of ampicillin, with shaking at 37 °C until the OD 600 value reached 0.8. The final concentration of 1 mM isopropyl β-D-1-thiogalactopyranoside (IPTG) was added to induce the protein expression at 20 °C overnight. Subsequently, the induced cells were harvested by centrifugation at 8000 rpm for 10 min and then lysed in lysis buffer (20 mM HEPES, pH 7.9, 500 mM KCl) by ultrasonication for 15 min. The insoluble pellets were separated by centrifugation at 15 000 rpm for 45 min. The supernatant was loaded on the Ni-NTA column and finally eluted with lysis buffer containing a gradient of imidazole from 10 mM to 500 mM.

MALDI-TOF mass spectrometry analysis of the αHL protein

All MALDI-TOF-MS data were acquired using a nitrogen laser (337 nm). The protein samples were prepared using a conventional dried droplet protocol and sinapic acid (SA) was used as the matrix. The sample (10 μL) was mixed with 10 μL of the SA matrix (1 : 1) and then 1 μL of this mixture was deposited on the MALDI sample stage. The difference in molecular weight between the wild-type αHL and the mutant $(E111R/K147R)_7$ αHL protein indicated that we have obtained the mutant $(E111R/K147R)_7$ αHL protein successfully.

The isothermal titration calorimetry (ITC) of CP[5]A and PQ

To evaluate the thermodynamic parameters of the interactions between CP[5]A and PQ, ITC experiments were performed by a MicroCal ITC 200 at 25 °C in ddH_2O. CP[5]A was dissolved in 1 mL of ddH_2O under ultrasonication to reach a concentration of 0.1 mM. PQ was dissolved in 1 mL of ddH_2O to reach a concentration of 1 mM. First, 0.1 mM of CP[5]A solution was placed in 300 μL of the sample cell of the calorimeter, while 1 mM of the PQ solution was loaded using the 50 μL injection syringe. Then, the PQ solution was titrated using the sample cell at a sequence of 25 injections of 2 μL aliquots with an

interval of 120 s. The contents of the sample cell were stirred at 1000 rpm throughout the measurements to ensure thorough mixing. Calorimetric data were analysed using OriginPro software and Origin 9.1 software. The raw data were analysed to obtain the binding stoichiometry (N), affinity constant (K), and other thermodynamic parameters of the reaction.

Electrophysiology recording and data analysis

All electrophysiology results were acquired using a BC-535 patch clamp amplifier and were digitized using a Digidata 1550 B1 digitizer (Molecular Devices, UK). 1,2-Diphytanoyl-*sn*-glycero-3-phosphocholine (DphPC) was used to form a lipid bilayer to seal the orifice, and the capacitance shown as 80–120 pF indicated that good lipid bilayers were formed. This lipid bilayer divides the chamber into *cis* and *trans* compartments both filled with 1 mL of 1.5 M KCl buffer (1.5 M KCl, 20 mM HEPES, pH 7.0). Single channel recordings were performed at 24 ± 1 °C. A pair of Ag/AgCl electrodes were placed in the *cis* and *trans* sides of the chamber, connected with the aqueous buffer, respectively. An appropriate amount of the mutant $(E111R/K147R)_7$ αHL nanopore solution was added to the *cis* side to form the stable single nanopore used in the following experiments. The acquired single channel data were sampled at a frequency of 20 kHz and filtered with a frequency of 1 kHz. Event states were detected by the single channel search feature in Clampfit 11.03 and further analysed by Origin 9.1 (Origin Lab).

Conclusions

In summary, we reported a highly sensitive αHL nanopore sensor in which CP[5]A acted as the aptamer for the detection of PQ at the single-molecule level. By taking advantage of the non-covalent interaction, the water-soluble host molecule – CP[5]A, was lodged into the restriction of the αHL nanopore. In addition, by introducing the positively charged arginine (Arg) into residues 111 and 147 of the αHL nanopore, we enhanced the interaction between CP[5]A and the nanopore and then improved the stability of the nanopore sensor. Importantly, our nanopore sensor could detect PQ even at concentrations as low as 2 nM and compared to conventional instrumental analytical methods in PQ detection, such as fluorescence sensing, high-performance liquid chromatography and capillary electrophoresis, the sensor platform that we have developed shows high sensitivity. Meanwhile, based on the National Food Safety Standard of China (GB 2763.1-2018), the LOD for PQ of our nanopore sensor was measured to be lower by two orders of magnitude than the MRL. The results in this paper may be inspiring and instructive in the design of the αHL nanopore sensor, which can serve as the single-molecule tool in the investigation of other small analytes.

Conflicts of interest

There are no conflicts of interest to declare.

Acknowledgements

This work was supported by the National Key R&D Program of China (Grant No. 2018YFA0901600 and 2020YFA0908500) and the Natural Science Foundation of China (Grant No. 22001054 and 22075065).

Notes and references

1 S. O. Igbedioh, Effects of agricultural pesticides on humans, animals, and higher-plants in developing-countries, *Arch. Environ. Health*, 1991, **46**, 218–224.
2 L. Rani, K. Thapa, N. Kanojia, N. Sharma, S. Singh, A. S. Grewal, A. L. Srivastav and J. Kaushal, An extensive review on the consequences of chemical pesticides on human health and environment, *J. Cleaner Prod.*, 2021, **283**, 124657.
3 F. Laghrib, M. Bakasse, S. Lahrich and M. A. El Mhammedi, Electrochemical sensors for improved detection of paraquat in food samples: a review, *Mater. Sci. Eng., C*, 2020, **107**, 110349.
4 S. H. Wang, L. J. Zhang, X. Q. Wang, Z. Y. Wang, C. C. Wen, J. S. Ma, Z. M. Gao and L. F. Hu, Metabolic changes in rat lung after acute paraquat poisoning by gas chromatography-mass spectrometry, *Int. J. Clin. Exp. Med.*, 2016, **9**, 21514–21520.
5 R. Gill, S. C. Qua and A. C. Moffat, High-performance liquid chromatography of paraquat and diquat in urine with rapid sample preparation involving ion-pair extraction on disposable cartridges of octadecyl-silica, *J. Chromatogr.*, 1983, **255**, 483–490.
6 Z. Pourghobadi, H. Makanali and H. Zare, Highly Sensitive Fluorescent Probe for Detection of Paraquat Based on Nanocrystals, *J. Fluoresc.*, 2021, **31**, 559–567.
7 H. C. Wu and H. Bayley, Single-molecule detection of nitrogen mustards by covalent reaction within a protein nanopore, *J. Am. Chem. Soc.*, 2008, **130**, 6813–6819.
8 M. Y. Li, Y. L. Ying, S. Li, Y. Q. Wang, X. Y. Wu and Y. T. Long, Unveiling the Heterogenous Dephosphorylation of DNA Using an Aerolysin Nanopore, *ACS Nano*, 2020, **14**, 12571–12578.
9 Y. Long and M. Zhang, Self-assembling bacterial pores as components of nanobiosensors for the detection of single peptide molecules, *Sci. China: Chem.*, 2009, **52**, 731–733.
10 J. Cao, S. Zhang, J. Zhang, S. Wang, W. Jia, S. Yan, Y. Wang, P. Zhang, H. Y. Chen and S. Huang, A Single-Molecule Observation of Dichloroaurate(I) Binding to an Engineered Mycobacterium smegmatis porin A (MspA) Nanopore, *Anal. Chem.*, 2021, **93**, 1529–1536.
11 Q. Liu, K. Xiao, L. P. Wen, Y. Dong, G. H. Xie, Z. Zhang, Z. S. Bo and L. Jiang, A Fluoride-Driven Ionic Gate Based on a 4 Aminophenylboronic Acid-Functionalized Asymmetric Single Nanochannel, *ACS Nano*, 2014, **8**, 12292–12299.
12 C. Yang, L. Liu, T. Zeng, D. Yang, Z. Yao, Y. Zhao and H. C. Wu, Highly Sensitive Simultaneous Detection of

Lead(II) and Barium(II) with G Quadruplex DNA in alpha-Hemolysin Nanopore, *Anal. Chem.*, 2013, **85**, 7302–7307.

13 Y. L. Guo, F. F. Jian and X. F. Kang, Nanopore sensor for copper ion detection using a polyamine decorated beta-cyclodextrin as the recognition element, *RSC Adv.*, 2017, **7**, 15315–15320.

14 X. F. Kang, S. Cheley, X. Guan and H. Bayley, Stochastic detection of enantiomers, *J. Am. Chem. Soc.*, 2006, **128**, 10684–10685.

15 W. J. Ramsay and H. Bayley, Single-Molecule Determination of the Isomers of D-Glucose and D-Fructose that Bind to Boronic Acids, *Angew. Chem., Int. Ed.*, 2018, **57**, 2841–2845.

16 X. H. Chen, G. M. Roozbahani, Z. J. Ye, Y. W. Zhang, R. Ma, J. L. Xiang and X. Y. Guan, Label-Free Detection of DNA Mutations by Nanopore Analysis, *ACS Appl. Mater. Interfaces*, 2018, **10**, 11519–11528.

17 Y. Astier, O. Braha and H. Bayley, Toward single molecule DNA sequencing: direct identification of ribonucleoside and deoxyribonucleoside 5′-monophosphates by using an engineered protein nanopore equipped with a molecular adapter, *J. Am. Chem. Soc.*, 2006, **128**, 1705–1710.

18 Q. Zhao, R. S. S. de Zoysa, D. Wang, D. A. Jayawardhana and X. Guan, Real-Time Monitoring of Peptide Cleavage Using a Nanopore Probe, *J. Am. Chem. Soc.*, 2009, **131**, 6324–6325.

19 A. F. Hammerstein, S. H. Shin and H. Bayley, Single-Molecule Kinetics of Two-Step Divalent Cation Chelation, *Angew. Chem., Int. Ed.*, 2010, **49**, 5085–5090.

20 T. Ogoshi, S. Kanai, S. Fujinami, T. A. Yamagishi and Y. Nakamoto, *para*-Bridged Symmetrical Pillar[5]arenes: their Lewis Acid Catalyzed Synthesis and Host–Guest Property, *J. Am. Chem. Soc.*, 2008, **130**, 5022–5023.

21 N. Song and Y. W. Yang, Applications of pillarenes, an emerging class of synthetic macrocycles, *Sci. China: Chem.*, 2014, **57**, 1185–1198.

22 Y. Yao, M. Xue, X. Chi, Y. Ma, J. He, Z. Abliz and F. Huang, A new water-soluble pillar[5]arene: synthesis and application in the preparation of gold nanoparticles, *Chem. Commun.*, 2012, **48**, 6505–6507.

23 S. Fu, Y. Zhang, S. W. Guan, Q. X. Huang, R. B. Wang, R. Z. Tian, M. S. Zang, S. P. Qiao, X. Zhang, S. D. Liu, X. T. Fan, X. M. Li, Q. Luo, C. X. Hou, J. Y. Xu, Z. Y. Dong and J. Q. Liu, Reductive-Responsive, Single Molecular-Layer Polymer Nanocapsules Prepared by Lateral Functionalized Pillar 5 arenes for Targeting Anticancer Drug Delivery, *ACS Appl. Mater. Interfaces*, 2018, **10**, 14281–14286.

24 S. Fu, G. An, H. C. Sun, Q. Luo, C. X. Hou, J. Y. Xu, Z. Y. Dong and J. Q. Liu, Laterally functionalized pillar 5 arene: a new building block for covalent self-assembly, *Chem. Commun.*, 2017, **53**, 9024–9027.

25 H. Li, D. X. Chen, Y. L. Sun, Y. B. Zheng, L. L. Tan, P. S. Weiss and Y. W. Yang, Viologen-Mediated Assembly of and Sensing with Carboxylatopillar 5 arene-Modified Gold Nanoparticles, *J. Am. Chem. Soc.*, 2013, **135**, 1570–1576.

26 Z. Zhang, Y. Luo, J. Chen, S. Dong, Y. Yu, Z. Ma and F. Huang, Formation of Linear Supramolecular Polymers That Is Driven by CH$\cdots\pi$ Interactions in Solution and in the Solid State, *Angew. Chem., Int. Ed.*, 2011, **50**, 1397–1401.

27 M. Xue, Y. Yang, X. Chi, Z. Zhang and F. Huang, Pillararenes, A New Class of Macrocycles for Supramolecular Chemistry, *Acc. Chem. Res.*, 2012, **45**, 1294–1308.

28 J. Y. Chen, Q. Xiao, H. Behera and J. L. Hou, Unimolecular artificial transmembrane channel with terminal dihydrogen phosphate groups showing transport selectivity for ammonium, *Chin. Chem. Lett.*, 2020, **31**, 77–80.

29 W. Si, L. Chen, X. B. Hu, G. Tang, Z. Chen, J. L. Hou and Z. T. Li, Selective Artificial Transmembrane Channels for Protons by Formation of Water Wires, *Angew. Chem., Int. Ed.*, 2011, **50**, 12564–12568.

30 Z. J. Yan, D. D. Wang, Z. J. Ye, T. Fan, G. Wu, L. Y. Deng, L. Yang, B. X. Li, J. W. Liu, T. H. Ma, C. Q. Dong, Z. T. Li, L. H. Xiao, Y. F. Wang, W. N. Wang and J. L. Hou, Artificial Aquaporin That Restores Wound Healing of Impaired Cells, *J. Am. Chem. Soc.*, 2020, **142**, 15638–15643.

31 L. L. Tan and Y. W. Yang, Molecular recognition and self assembly of pillarenes, *J. Inclusion Phenom. Macrocyclic Chem.*, 2015, **81**, 13–33.

32 T. Ogoshi, M. Hashizume, T. A. Yamagishi and Y. Nakamoto, Synthesis, conformational and host–guest properties of water soluble pillar[5]arene, *Chem. Commun.*, 2010, **46**, 3708–3710.

33 G. Miles, H. Bayley and S. Cheley, Properties of Bacillus cereus hemolysin II: a heptameric transmembrane pore, *Protein Sci.*, 2002, **11**, 1813–1824.

